

CLOSE NEIGHBORS OF MARKARIAN GALAXIES

II. STATISTICS AND DISCUSSIONS

T. A. Nazaryan¹, A. R. Petrosian¹, A. A. Hakobyan¹, B. J. McLean², and D. Kunth³

¹ Byurakan Astrophysical Observatory, Armenia; e-mail: nazaryan@bao.sci.am

² Space Telescope Science Institute, USA

³ Institut d'Astrophysique de Paris, France

According to the database from the first paper, we select 180 pairs with $dV < 800 \text{ km s}^{-1}$ and $D_p < 60 \text{ kpc}$ containing Markarian (MRK) galaxies. We study the dependence of galaxies integral parameters, star-formation (SF) and active galactic nuclei (AGN) properties on kinematics of pairs, their structure and large-scale environments. Following main results were obtained: projected radial separation D_p between galaxies correlates with the perturbation level P of the pairs. Both parameters do not correlate with line-of-sight velocity difference dV of galaxies. D_p and P are better measures of interaction strength than dV . The latter correlates with the density of large-scale environment and with the morphologies of galaxies. Both galaxies in a pair are of the same nature, the only difference is that MRK galaxies are usually brighter than their neighbors in average by 0.9 mag. Specific star formation rates (SSFR) of galaxies in pairs with smaller D_p or dV is in average 0.5 dex higher than that of galaxies in pairs with larger D_p or dV . Closeness of a neighbor with the same and later morphological type increases the SSFR, while earlier-type neighbors do not increase SSFR. Major interactions/mergers trigger SF and AGN more effectively than minor ones. The fraction of AGNs is higher in more perturbed pairs and pairs with smaller D_p . AGNs typically are in stronger interacting systems than star-forming and passive galaxies. There are correlations of both SSFRs and spectral properties of nuclei between pair members.

Key words: galaxies: general – galaxies: interactions – galaxies: starburst – galaxies: active – galaxies: peculiar

1 Introduction

Close interactions/mergers of galaxies are considered as important processes influencing morphological, stellar and chemical evolution of galaxies. Numerous observational results show that interactions/mergers trigger SF in galaxies. The pioneering work [1] showed that peculiar galaxies have wider spread on color-color diagram and, generally, are bluer than normal galaxies. The authors suggested that sharp bursts of SF, with their timescales consistent with interactions, can explain peculiar colors of these galaxies. Later, many others showed that closer pairs of galaxies have enhanced star formation rates (SFRs) measured by emission lines, e.g. [2,3,4,5], optical colors, e.g. [6,7], infrared (IR) emission, e.g. [8,9], supernovae distribution, e.g. [10,11]. The main physical processes responsible for the enhanced SF are gas inflow toward nuclear regions of galaxies due to global torques and, probably, gas fragmentation into massive and dense clouds and rapid SF therein, e.g. [12,13]. The triggering mechanism of AGN is often considered to be the same as that of the enhanced nuclear SF [5,14,15,16,17].

In spite of that, various aspects and many factors can affect on frequency and efficiency of enhanced SF triggering by galaxy interaction and merging. The role of large-scale environment is still debated, especially, taking into account morphology-density relation [18]. In this respect, in [19,20] it was observed that galaxy interactions are more effective in triggering SF in low- and moderate-density environments. In addition, in [8,21] it was found that late-type neighbors enhance SF of galaxies while early-type neighbors reduce it, and it was showed that the role of the large-scale density in determining galaxy properties is minimal once luminosity and morphology are fixed. On the other hand, effect of large-scale environment was considered small, but non-zero in [22]. It is mostly assumed that major mergers are more effective in triggering starbursts (also AGNs), than minor ones [4,5,14,16,23,24,25,26]. At the same time, minor mergers occur more frequently, and partially can explain triggered SF in early-type galaxies, e.g. [27,28].

Finally, the general role of interactions and mergers in triggering SF of galaxies is still not clear. The facts, that not all galaxies with high SFR are interacting ones, as well as that not all interacting galaxies have high SFR, support the hypothesis that internal properties of galaxies are also an important factor determining enhanced SF [3,19], especially at higher redshifts [29,30]. Bars, transferring gas to nuclei, can be an alternative mechanism of induced nuclear SF [31,32], although bars themselves are disputably considered to be interaction-induced, e.g. [33].

The large variety of parameters is one of the main difficulties in studying influence of interactions and mergers on SF and AGN properties of galaxies. The choice of galaxies as interacting also contains some ambiguities, because interacting pairs can be selected by different criteria, such as according to the difference of line-of-sight (LoS) velocity, projected distance between pair members, or the degree of morphological disturbances (assessed both visually or automatically, e.g. by asymmetry). Although these parameters are correlated with each other at first approximation, see e.g. [26,34], they can bias the pair statistics in different ways because of correlation with large-scale environment, e.g. [20], possible effects on morphological classification, e.g. [33], or different timescales and sequences of SF, AGN and disturbed morphology [5,6,13,35]. The sizes of samples also vary greatly in different studies, from several hundreds to a hundred thousand [4], bringing additional difficulties for making satisfactory conclusions. Additional, scrupulously chosen samples can provide further results to reveal the details.

The aim of this study is to investigate the connections between gravitational interaction with a close neighbor and nuclear activity and/or enhanced SF in galaxy pairs. We will study these phenomena through examining dependence of integral parameters, SFRs and nuclear properties of galaxies in pairs on kinematical properties of these systems, as well as their largescale environments. Also, we will investigate correlations between properties of paired galaxies.

In our first paper of a series [36], we have reported the creation of the database of close neighbors of MRK galaxies, which contains extensive new measurements of their optical parameters, collected near-IR data, and pair properties. This is a second paper of a series and the outline is as follows: Sect. 2 presents the sample of close pairs of galaxies and selected parameters. Section 3 presents the statistical study of the sample and discusses its results. Section 4 is the summary of this study. Throughout this paper, we adopt the Hubble constant $H_0 = 73 \text{ km s}^{-1} \text{ Mpc}^{-1}$.

2 The sample

There are two possible approaches for pair selection with the purposes of studying SF and AGN properties of pair members. First, one can select all pairs from a catalog of galaxies and study SF and AGN properties in these pairs. Second, one can choose only galaxies with desirable properties, search for their neighbors and study properties of these pairs. The first approach is more commonly used, e.g. in [16], because it provides selection of pairs with all possible variety of parameters and is limited only by original catalogs of galaxies drawn from. The second approach (e.g. used in [17]) gives an opportunity to select a well-chosen sample of pairs, which generally will be smaller, but the selection effects should be constrained in a comprehensible manner. We adopt the second approach in our pair selection. It gives us an opportunity to select well-chosen sample containing enough number of galaxies with different activity levels, but small enough to study it thoroughly via visual classification and manual checking of automatically measured parameters.

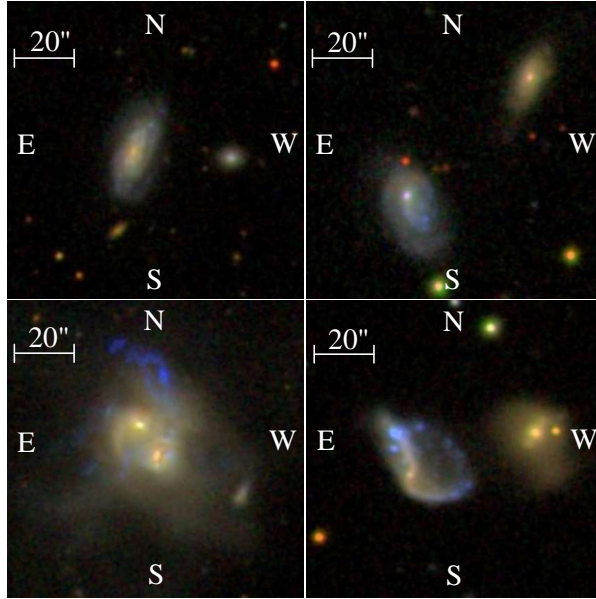


Fig. 1 Examples of pairs with perturbation levels $P = 0$ (top left), $P = 1$ (top right), $P = 2$ (bottom right), and $P = 3$ (bottom left).

The starting point to create our sample of pairs is the catalog of MRK galaxies. The original catalog [37] features 1545 bright galaxies mostly having starburst properties and/or AGNs, which are well-studied objects. In [38], homogeneously measured parameters of MRK galaxies, such as magnitudes, sizes, positions, redshifts, and morphologies, are presented.

Results of a close neighbors search for MRK galaxies within position-redshift space using the NASA/IPAC Extragalactic Database and Sloan Digital Sky Survey (SDSS) Data Release (DR) 8 (for current study we added to this list some new objects found only in the DR9 [39]) are published in [36]. In [36], three criteria were used to select the sample of close neighbors of MRK galaxies. (1) Redshift of MRK galaxy should be more than 0.005. (2) Difference of LoS velocities of MRK galaxy and its neighbor should be less than 800 km s^{-1} . (3) Projected distance between MRK galaxies and their neighbors should be less than 60 kpc (close systems). According to these criteria, 633 galaxies in close systems containing 274 MRK galaxies were found. For the current study, only pairs of galaxies were selected from above mentioned 633 galaxies. The total number of pairs containing at least one MRK galaxy is 217. The percentage of pairs in our sample located within the SDSS coverage is 83 %. The median distance of selected pairs is 96 Mpc.

The morphological classification of MRK galaxies and their neighbors was done in [38] and [36] respectively, using only Digitized Sky Survey-II (DSS-II) blue and red images for MRK and DSS-II blue and red images as well SDSS color images for neighbors. For this study, we check morphological classes of MRK galaxies by using also SDSS color images for homogeneity. New and revised morphological classes were suggested for the 16 % of MRK galaxies, morphological classes were specified for other 17 % of galaxies. The 19 % of sample galaxies are of early-types (earlier than S0/a), 46 % of early spirals (Sa-Sbc), and 36 % of late spirals and irregulars (later than Sc).

We classified sample pairs in terms of morphological perturbations, e.g. [17,26], by 4 levels: $P = 0$: unperturbed pairs, $P = 1$: slightly perturbed, $P = 2$: highly perturbed, $P = 3$: mergers. Unperturbed pairs are defined as having both components with no visible morphological perturbation. Slightly perturbed pairs are pairs where the most perturbed component has visible morphological perturbations, but without long tidal arms, bridges, or violation of spiral patterns or brightness profile. In highly perturbed pairs the most perturbed component has significant morphological perturbations, such as long tidal arms, bridges, or violation of spiral patterns or brightness profile. Mergers are pairs with obvious merging processes. The typical examples of pairs of each category are shown in Fig. 1. The 45 % of

the pairs have $P = 0$, 23 % $P = 1$, 22 % $P = 2$, and 10 % $P = 3$. Blind reclassification of a sample shows that the selection criteria for perturbation are quite reliable and objective, and errors of this classification are less than errors of morphological t -types classification. Typically less than 20 % of pairs change their P level by one unit when reclassified.

In [36,38], isophotal magnitudes of the galaxies from DSS-II blue (J), red (F), and near-IR (I) images were measured in an homogeneous way. In this study we used SDSS *cmodel* magnitudes for luminosities and *model* magnitudes for colors, which were controlled by DSS magnitudes (outliers were removed).

We describe the large-scale environments of each pair by average large-scale density Σ calculated as a surface density of galaxies from SDSS within 1 Mpc projected circles and with LoS velocity differences less than 1500 km s^{-1} (typical Σ of galaxy groups is less than 500 km s^{-1} [40]). For that purpose, we counted all galaxies in absolute magnitude limited sample $M \leq -18.74$ in r -band corresponding to SDSS completeness magnitude $r_{\text{Petro}} < 17.77$ [41] at 200 Mpc distance (95 % of pairs are closer). So 95 % of pairs do not lose galaxies in their 1 Mpc environments because of magnitude limit. In higher density environments there is a systematic undercount of neighbors due to fiber collisions [41]. We complete number of neighbor galaxies proportionally to not-covered area for 17 pairs having 1 Mpc circles partially located outside of SDSS coverage. For our further statistics we divide all pairs according to Σ into three categories: low-, medium-, and high-density environments with $\Sigma \leq 2$, $2 < \Sigma \leq 5$, and $\Sigma > 5$ accordingly.

For statistics we also included some spectral parameters of galaxies processed by MPA-JHU pipeline, which fits galaxy templates and spectral synthesis models to the spectra [42,43]. These parameters are SFR and SSFR for whole galaxy, and nuclear emission-line classification. We visually inspected each galaxy in our sample and filtered only those having nucleus located within SDSS spectral fiber. Mean values of $\log(\text{SFR})$ and $\log(\text{SSFR})$ are -0.1 ± 0.8 and -9.9 ± 0.9 for MRK and -0.7 ± 0.9 and -10.1 ± 0.9 for neighbors.

We divide galaxies of our sample into four groups basing on nuclear BPT [44] classification of their SDSS spectra. These classes are BPT = PS for passive nuclei (which are not included in BPT classification); BPT = SF for star-forming nuclei; BPT = C for composite nuclei, BPT = AGN for Seyfert galaxies, and BPT = L for LINERs. The 9 ± 2 % of galaxies out of 180 with available spectra have passive, 66 ± 6 % have star-forming, 14 ± 3 % have composite, 2 ± 1 % have AGN, and 8 ± 1 % have LINER nuclei. Surprisingly, we found 7 cases when the nucleus of MRK galaxy has spectral classification “passive”. These galaxies are: MRKs 422, 562, 654, 842, 902, 1276, and 1349. We inspected their SDSS spectra and found that only MRK 654 has emission lines and can have typical spectrum of starburst galaxy. All the other cases are early-type galaxies with neither excess in blue band nor any strong emission lines.

We study some possible selection effects of the sample that could bias further statistics. The dependence of absolute magnitude on redshift (*Malmquist* bias) is quite strong in the sample: $M_r = -18.45 - 0.0137 d$; (correlation coefficient $r = -0.50$), where d is the distance from us in Mpc. As a result, morphologies of galaxies are also biased by distance: $d = 111 \pm 67$ Mpc for early-types, $d = 119 \pm 59$ Mpc for early spirals, and $d = 82 \pm 42$ Mpc for late spirals and irregulars. Other morphological features, i.e., perturbation levels of pairs and bar detection, are not biased by distance. Kinematical parameters of pairs, i.e. dV and Dp are also not biased by distance. Because of sample selection criteria, we have deficit of passive-passive pairs and, to a lesser extent, active-passive pairs.

3 Statistics and discussions

3.1 Multivariate factor analysis (MFA)

The statistical research was conducted in two steps. First, we applied an exploratory MFA to look for correlations between all parameters describing MRK galaxies, their neighbors (t -type, bar, abs. mag, $B - R$, SSFR, and BPT type) and pair properties (dV , Dp , P , and Σ). This statistical method is similar to the more commonly used principal component analysis. The MFA describes the interdependence and grouping patterns of variables in terms of factors. Factor loadings are measures of involvement of variables in factor patterns and can be interpreted like correlation coefficients. The square of the loading

Table 1 Varimax rotated normalized orthogonal factor loadings.

Variable	F_1	F_2	F_3
dV	-0.51	0.06	-0.09
D_p	-0.11	0.48	-0.09
P	-0.11	-0.75	0.31
Σ	-0.42	0.39	0.15
t -type MRK	0.80	0.04	0.21
Bar MRK	0.16	0.30	0.36
M MRK	0.70	0.43	0.12
$B - R$ MRK	-0.53	0.12	-0.16
SSFR MRK	0.71	-0.02	0.13
BPT MRK	0.07	-0.54	-0.23
t -type Neig.	0.77	-0.05	-0.27
Bar Neig.	-0.02	-0.05	0.72
M Neig.	0.61	0.42	-0.38
$B - R$ Neig.	-0.49	0.29	0.54
SSFR Neig.	0.77	-0.14	-0.30
BPT Neig.	0.12	-0.11	-0.47
Accum. variance	26 %	38 %	49 %

is the variation that a variable has in common with the factor pattern. The percent of total variance carried by a factor is the mean of squared loadings for a factor. In order to simplify the interpretation of the results, we only present the rotated varimax normalized orthogonal values for the three most significant factors, with highlighted values above 0.4 correlation threshold. Table 1 shows the factor loadings, i.e., the correlation coefficients between the initial variables and the factors for the $N = 59$ subsample with known values of all initial variables of galaxies.

Factor F_1 is the combination of LoS velocity difference dV, density of environment Σ and t -types, abs. mag, colors, SSFRs of MRK and neighbor galaxies. Pairs with smaller dV and in less denser environments have preferably fainter and bluer galaxies of later morphological types and with higher SSFRs. Factor F_2 is the combination of pair perturbation levels P , D_p separation, abs. mag of MRK and neighbor galaxies, BPT classification of MRK galaxy. MRK galaxies with active nuclei are located in closer and more perturbed pairs, they and their neighbors are relatively luminous galaxies. Factor F_3 connects bar existence, color and nuclear activity of neighbor galaxies. Redder neighbor galaxies have larger fraction of bars and active nuclei. These results are expected, they show common trends connecting properties of galaxies and their environments [16, 18, 20].

3.2 Sample properties

An important goal of this study is to examine the dependence of SSFR and BPT types (target parameters) on dV, D_p and P (primary parameters) taking into account the impact of secondary parameters such as morphologies, large-scale environments, luminosity ratio of pair components. In this section we mention some other important relations (between primary and secondary parameters) that are essential to consider when discussing the sample properties. The dependence of visually detected perturbation level P on dV and D_p is worthy to mention. Figure 2 shows the distribution of pairs by their dV and D_p , pairs with different perturbation levels P are marked. It is obvious and shown by MFA too, that P correlates only with D_p , while dV and D_p do not correlate with each other. The closer pairs are more disturbed. This is the result of different nature of D_p and dV. Pairs with larger dV correspond to environments with higher densities Σ . Therefore while D_p is a measure of interaction strength, the variation of dV mainly reflects change of large-scale environments.

The fraction of barred galaxies in the sample depends neither on morphological type (after removing elliptical and irregulars) nor on D_p . On the other hand, there is a strong decrease of number of barred

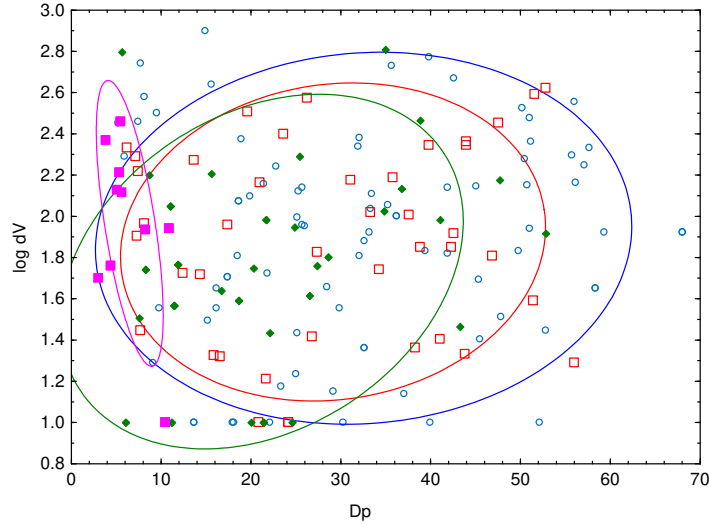


Fig. 2 D_p vs. $\log(dV)$ for all pairs with different levels of perturbation P . $P = 0$ are marked by blue small blank circles, $P = 1$ by red large blank squares, $P = 2$ by green small filled diamonds, $P = 3$ by purple large filled squares. Ellipses correspond to 95 % of points of each distribution.

galaxies from 47 ± 10 % for small dV ($10 - 20 \text{ km s}^{-1}$) pairs to 14 ± 3 % for large dV ($> 100 \text{ km s}^{-1}$) pairs. The SSFRs of barred galaxies do not differ from those of unbarred ones significantly.

3.3 MRK galaxies vs. neighbors

We compared properties of neighbors with those of MRK galaxies. Mean absolute *cmodel* r mag of neighbors is -19.4 ± 1.8 compared to -20.3 ± 1.2 for MRK galaxies. Median morphological type of neighbor galaxy is Sbc compared to Sb for MRK galaxy. A Kolmogorov-Smirnov (KS) test of morphologies gives $p = 0.09$ that MRK and neighbors are drawn from the same sample. Spearman's rank ($R = 0.29$) test shows that the morphologies of MRK and neighbors correlate significantly ($p = 0.00005$). Number of barred galaxies in neighbors sample is 23 ± 4 % compared to 22 ± 3 % for that in MRK galaxies. Comparison of SSFRs shows that SSFR of neighbors is not less than that of MRK galaxies. The distribution of neighbors by BPT types is consistent with the distribution of MRK galaxies. A KS test shows that the distribution of neighbors by colors is statistically the same as that of MRK galaxies. Therefore neighbor galaxies are of the same nature as MRK galaxies. We consider this fact as a result of existence of correlation between properties of galaxies in pairs. Because of magnitude limitation of Markarian survey [37], MRK galaxies are usually the brightest members of pairs and are brighter in average by 0.9 mag.

3.4 Dependence of SSFR on the parameters of interaction

The main parameters describing interactions are dV , D_p , and P . Figure 3 shows the dependence of SSFR on dV of a pair. We remove galaxies with AGNs, then categorize the rest by morphologies to make adequate comparison. Figure 3 shows that, without considering morphologies, we see 0.7 dex increase of SSFRs from larger dV to smaller ones. However the variance of SSFRs because of morphologies is much larger (more than 2.5 dex). In [20], it was shown that dV is biased by large-scale environment: pairs in denser environments have larger dV . Because of morphology–density relation, dV is also biased by morphologies: early-type galaxies have $dV \sim 250 \text{ km s}^{-1}$ while irregulars have $dV \sim 70 \text{ km s}^{-1}$, so most of the SSFR vs. dV dependence is because of morphology–SSFR dependence and does not reflect

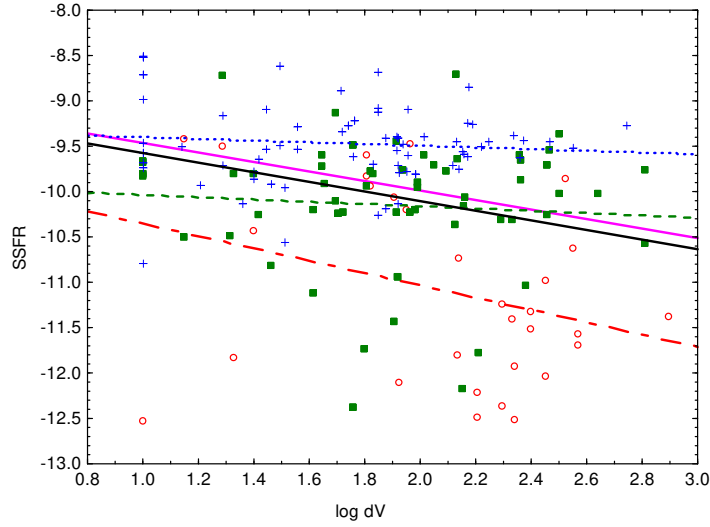


Fig. 3 SSFR vs. $\log(dV)$ for subsamples of early-types (red blank circles, dashed-dotted line), early spirals (green filled squares, dashed line), and late spirals and irregulars (blue crosses, dotted line). Two best-fit lines for all galaxies (black bottom solid line) and AGN-removed sample (purple upper solid line) are drawn.

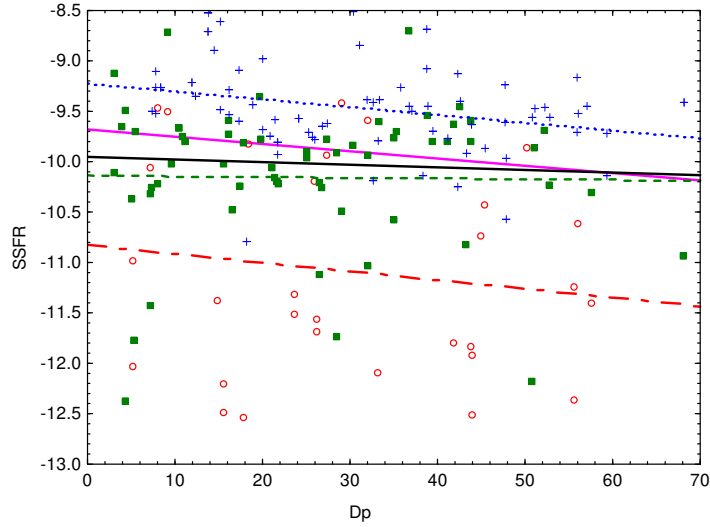


Fig. 4 SSFR vs. D_p grouped by morphologies. Points and lines marking are the same as in Fig. 3.

pure interaction. Thus, we conclude that it is essential to take into account morphologies of galaxies when discussing their SSFRs and interactions to obtain unbiased results. Figure 3 shows that grouping by morphologies weakens SSFR vs. dV relation, but there still remains some variance, which is maximal for early spirals ($0.4 - 0.5$ dex). This result is in agreement with modeling, e.g. [29] showing that strong starbursts during interactions are rare and that typical enhancement of SF is less than 5 times.

Figure 4 shows the dependence of SSFR on D_p of a pair in AGN-removed sample. If we do not categorize the sample by morphologies, we see 0.7 dex increase of SSFR from larger D_p to smaller ones. In our sample D_p is not biased by morphologies compared to dV . After grouping by morphologies we have about 0.5 dex difference of SSFRs in closer pairs compared to the wider ones. D_p correlates stronger with the perturbation level P than dV . Meanwhile, SSFRs correlate weakly with perturbation.

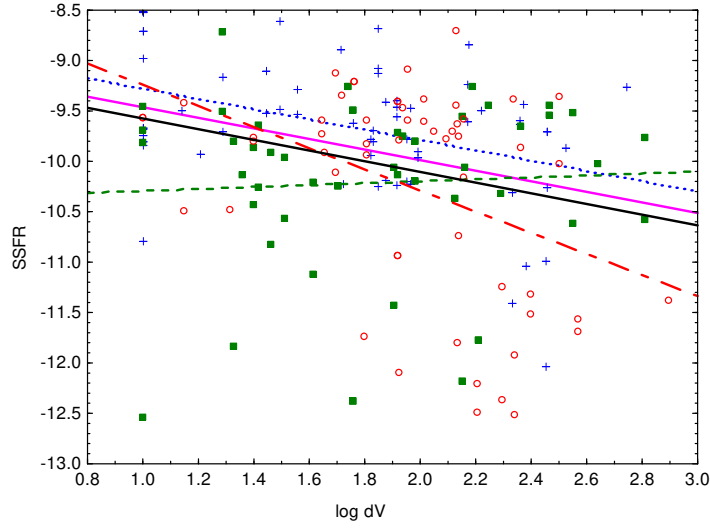


Fig. 5 SSFR vs. $\log(dV)$ for subsamples with large Σ (red blank circles, dashed-dotted line), medium Σ (green filled squares, dashed line), and low Σ (blue crosses, dotted line). Two best-fit lines for all galaxies (black bottom solid line) and AGN-removed sample (purple upper solid line) are drawn.

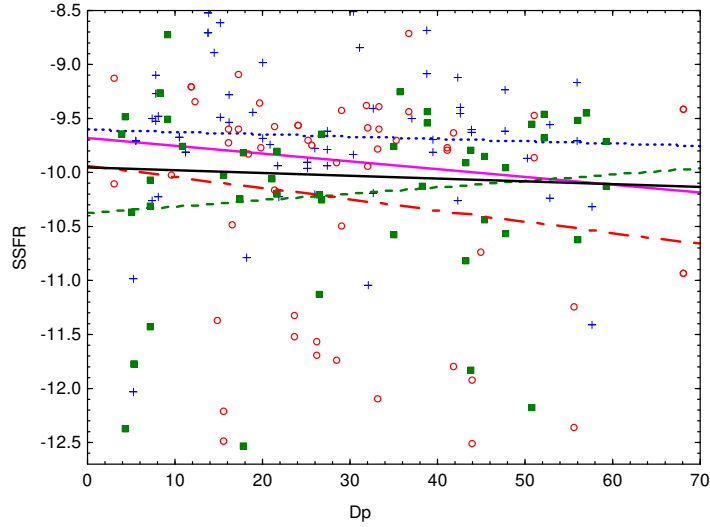


Fig. 6 SSFR vs. D_p grouped by large-scale density Σ . Points and lines marking are the same as in Fig. 5.

We interpret this partially as the result of two factors. First, P is biased by morphology: it is easier to detect disturbance of spiral galaxies, and more difficult when galaxy is of early-type or irregular. Second, peaks of SF usually coincide with pericenter passages according to models [29], however, the perturbations can be delayed.

The dependence of SSFR on dV grouped according to the density of large-scale environment Σ is shown in Fig. 5. There is an increase of SSFR for all environments by about 0.5 dex. We do not confirm the results in [19,20] which suggested stronger increase of SF in medium- and low-density environments than in high-density ones. The dependence of SSFR on D_p in environments with different Σ is shown in Fig. 6. There is no trend of SSFR increase in medium-density environments, while there is about 0.5 dex increase of SSFR in high-density environments and weaker trend in low-density ones. Binning

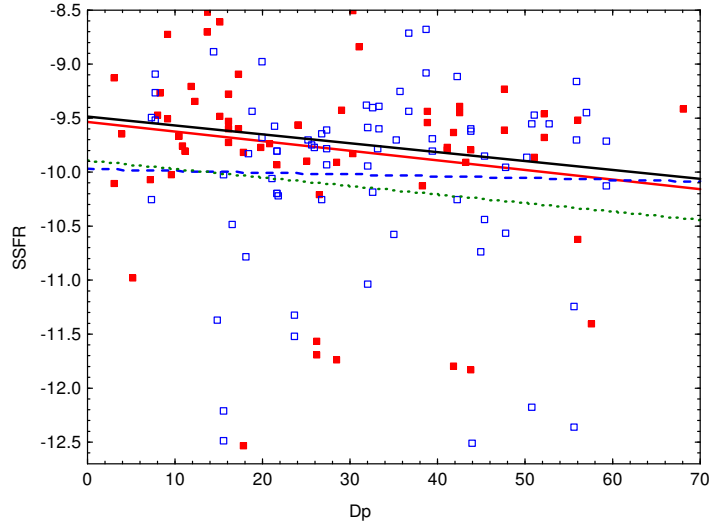


Fig. 7 SSFR vs. D_p for major interactions (red filled squares, solid line best fit), minor interactions (blue blank squares, dashed line), brightest components of major interactions (black upper solid line), and brightest components of minor interactions (green dotted line).

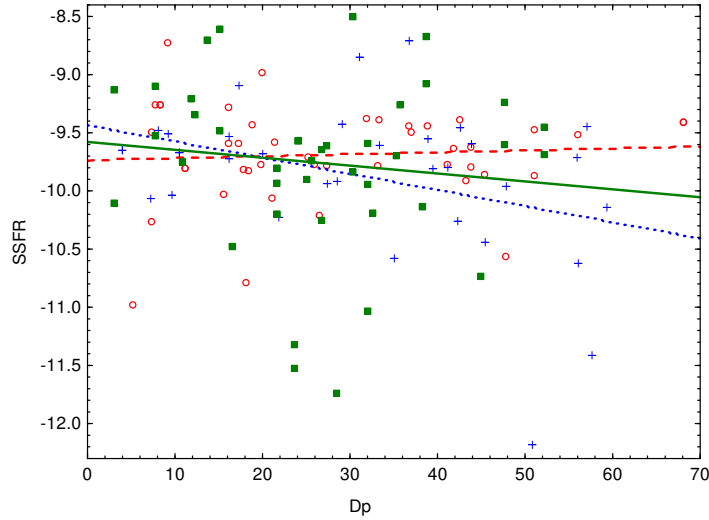


Fig. 8 SSFR vs. D_p for galaxies with relatively earlier type neighbors (red blank circles, dashed line), same type neighbors (green filled squares, solid line), and relatively later type neighbors (blue crosses, dotted line).

both by morphologies and large-scale environments in larger samples can make possible to separate the effects of morphologies and large-scale environment densities on SSFR increase. We tried also to group galaxies by their global colors instead of morphologies to see variations of SSFR vs. dV and D_p within each color group. However, there is no variation. This is probably because colors already depend on SSFR, and variation of color reflects variation of SF even within each morphological class.

We study the impact of the luminosity ratio of pair members on SSFR increase by dividing all the pairs into two categories. Those with $\log(L_{\text{bright}}/L_{\text{faint}}) \leq 0.6$ we call major interactions, and the rest we call minor ones (see also [3, 14, 24]). This separation is biased neither by redshift, nor by morphology or large scale environment. Figure 7 shows the SSFR– D_p relation for major and minor interactions, also the subsamples of the brightest members of pairs are showed separately. The major interactions are

more effective in triggering SF than minor ones, there is a 0.5 dex increase of SF in major interactions, while there is no trend among minor interactions. Figure 7 shows also that the brightest members of major interactions have higher SSFRs than pairs in average, therefore the brightest members obtain extra SSFR (if consider not-normalized SFR, it would be even more). This results are in agreement with previous both observational and modeling data [3,14,24,25,26] suggesting that tidal forces draw gas into the central regions of galaxies, and the merger mass ratio is an important parameter defining the effectiveness of the tidal forces.

The impact of morphology of neighbor galaxy on SSFR is shown in Fig. 8. Existence of earlier-type neighbor does not increase of SSFR, while the same-type and later-type neighbor increases SSFR of a galaxy. The extra SSFR is maximal if the neighbor galaxy is of later morphological type, in this case the SSFR increases by about 0.8 dex. Previous papers [8,21] also obtained similar result. This result supports the scenario where close interaction with a later type neighbor can not only trigger gas inflow in earlier type galaxy, but also be an additional source of gas fuel.

3.5 Nuclear types vs. pair properties

We study the fraction of galaxies with different nuclear BPT types by grouping the spiral galaxies in the sample according to the D_p and P . The fraction of AGN galaxies in less separated pairs is larger than that in more separated pairs. The difference is especially obvious when considering the perturbation level P . Fraction of AGNs changes from 8 % for unperturbed pairs ($P = 0$) to 55 % for mergers ($P = 3$) respectively. On the contrary, the fraction of star-forming galaxies changes from 69 % to 45 % in the same groups. This result (see also [16,23]) indicates that while both AGN and SF can be triggered by interactions, AGNs “prefer” stronger interactions. Different timings of starbursts and AGN events can explain this result [5,15,35].

The fraction of AGNs in barred spirals is not significantly different from that in spirals without bars. The fraction of AGNs in major interactions is about 4 times larger than that in minor ones (32 ± 7 % compared to 8 ± 5 %), showing results similar to [16].

3.6 Correlations between properties of pair members

We study whether there is a correlation between SSFRs of galaxies in a pair. First, we do this by grouping pairs according to the environments with the same large-scale density Σ . There are statistically significant correlations between SSFRs of pair members within low- and high-density environments ($p = 0.00003$ and $p = 0.0003$ respectively) with $r \sim 0.6$ correlation coefficient. Second, we also study correlation between SSFRs of galaxies in a pair, by filtering the same-morphology pairs and grouping them according to morphologies. The only statistically significant correlation we found is between SSFRs of galaxies within S0/a–Sab ($r = 0.95$, $p = 0.03$). In all the other groups of galaxies there is no any correlation. We explain the difference between these two results by the following reasons: the statistics by grouped morphologies has smaller sample than the statistics grouped by environments, and the correlations between enhanced SSFRs of pair members due to interactions are generally weak.

We study BPT–BPT correlations between pair members. For that purpose, we compare probability p_{ij} ($i, j = \text{passive, LINER, starforming, composite, AGN}$) with pure probability p_j , where p_{ij} is the conditional probability of a galaxy with BPT type i to have a neighbor with BPT type j , and p_j is probability for a random galaxy to have BPT type j . Table 2 shows the coupling coefficients $\gamma_{ij} = p_{ij}/p_j$. We calculated the variances of the coefficients by random generation of all possible pairs with mean numbers and standard deviations basing on existing numbers. For each spectral type, there is a tendency to have an increased probability of a neighbor with the same BPT type. Especially that is noticeable regarding passive galaxies and AGNs: passive galaxies are about 6 times more likely to be found near another passive galaxy, AGNs are 3 times more probable to be near another AGN. While our results suffer from low number statistics, we speculate that star-forming galaxies decrease the probability to have a passive, LINER or AGN neighbor. On the other hand, passive galaxies can increase the likelihood to have AGN or LINER neighbors. It is not difficult to calculate, that sample selection criteria does not decrease the diagonal coefficients, so these values in the Table 2 remain real for any sample (γ coefficient

Table 2 The coupling coefficients $\gamma_{ij} = p_{ij}/p_j$ with their variances, where i corresponds to the target galaxy, j to the neighbor.

Neighbor	Target				
	PS	L	SF	C	AGN
PS	5.6 ± 1.2	1.6 ± 1.2	0.3 ± 0.1	0.7 ± 0.4	1.6 ± 1.4
L	1.9 ± 1.5	1.3 ± 1.2	0.7 ± 0.3	0.9 ± 0.7	1.6 ± 1.5
SF	0.2 ± 0.1	0.8 ± 0.3	1.1 ± 0.1	0.8 ± 0.2	0.6 ± 0.4
C	0.6 ± 0.5	0.8 ± 0.7	0.9 ± 0.2	1.5 ± 0.5	1.0 ± 1.0
AGN	1.4 ± 1.1	1.5 ± 1.6	0.5 ± 0.3	1.7 ± 1.0	3.3 ± 3.2

of passive–passive pairs will be much more). Previous results showed that interaction-triggered SF and AGNs often are correlated between components in major interactions, e.g. [17, 25], and have tendency to appear in the environments of galaxies with similar properties, i.e. Seyfert galaxies tend to have the highest probability of having another Seyfert galaxy in the neighborhood, HII galaxies tend to have the highest probability of having another HII galaxy in the neighborhood, etc., e.g. [45]. We explain all the above mentioned correlations between BPT types as a result of two main factors. First, morphologies of galaxies are correlated: passive galaxies, AGNs and LINERs are more likely to be found among earlier type galaxies, while star-forming galaxies are more likely to be later type galaxies [46]. In this respect, correlation of morphologies between pair members automatically creates correlation of BPT types. Second, stronger interactions increase the likelihood of pair members to have nuclear activity of same types.

4 Summary

We studied pairs containing MRK galaxies, conducted both multivariate and one-dimensional statistics, and came to the following main conclusions:

- (i) Projected radial separation D_p between galaxies correlates with the perturbation level P of the pairs. Both parameters do not correlate with the LoS velocity difference dV of pair members. D_p and P are better measures of interaction strength than dV . The latter correlates with the density of large-scale environment and with the morphologies of galaxies.
- (ii) Both galaxies in a pair are of the same nature, the only difference is that MRK galaxies are usually brighter than their neighbors in average by 0.9 mag. This result supports the existence of correlation between properties of paired galaxies.
- (iii) SSFRs of galaxies in pairs with smaller D_p or dV is in average 0.5 dex higher than that of galaxies in pairs with larger D_p or dV . These trends are stronger when considering D_p , rather than dV and P . These trends exist within all groups selected by morphologies and within groups having low- and high-density environments.
- (iv) Major interactions/mergers trigger SF more effectively than minor ones. The brightest components of pairs gain more SSFR than the fainter ones. Closeness of a neighbor with same and later morphological type increases the SSFR, while earlier-type neighbors do not increase SSFR.
- (v) The fraction of AGNs is higher in more perturbed pairs and pairs with smaller D_p . AGNs typically are in stronger interacting systems than star-forming and passive galaxies. Major interactions/mergers trigger AGNs more effectively than minor ones.
- (vi) The correlations between SSFRs of pair members within fixed environments have medium strength. The correlations between SSFRs of pair members are weaker when considering same-morphology pairs. Galaxy with given nuclear spectral type tend to increase the probability of having a neighbor with similar nuclear properties. We suspect that the presence of passive galaxy reduces the probability to find a star-forming neighbor and increases the probability to find an AGN or LINER neighbor.

Acknowledgements

A.R.P. and A.A.H. acknowledge the hospitality of the Institut d’Astrophysique de Paris (France) during their stay as visiting scientists supported by the Collaborative Bilateral Research Project of the State Committee of Science (SCS) of the Republic of Armenia and the French Centre National de la Recherche Scientifique (CNRS). This work was made possible in part by a research grant from the Armenian National Science and Education Fund (ANSEF) based in New York, USA. This research made use of the NASA/IPAC Extragalactic Database, which is available at <http://ned.ipac.caltech.edu>, and operated by the Jet Propulsion Laboratory, California Institute of Technology, under contract with the National Aeronautics and Space Administration. Funding for SDSS-III has been provided by the Alfred P. Sloan Foundation, the Participating Institutions, the National Science Foundation, and the US Department of Energy Office of Science. The SDSS-III web site is <http://www.sdss3.org>. SDSS-III is managed by the Astrophysical Research Consortium for the Participating Institutions of the SDSS-III Collaboration including the University of Arizona, the Brazilian Participation Group, Brookhaven National Laboratory, University of Cambridge, Carnegie Mellon University, University of Florida, the French Participation Group, the German Participation Group, Harvard University, the Instituto de Astrofísica de Canarias, the Michigan State/Notre Dame/JINA Participation Group, Johns Hopkins University, Lawrence Berkeley National Laboratory, Max Planck Institute for Astrophysics, Max Planck Institute for Extraterrestrial Physics, New Mexico State University, New York University, Ohio State University, Pennsylvania State University, University of Portsmouth, Princeton University, the Spanish Participation Group, University of Tokyo, University of Utah, Vanderbilt University, University of Virginia, University of Washington, and Yale University.

REFERENCES

1. R. B. Larson and B. M. Tinsley, *Astrophys. J.*, **219**, 46, 1978.
2. E. J. Barton, M. J. Geller, and S. J. Kenyon, *Astrophys. J.*, **530**, 660, 2000.
3. D. G. Lambas, P. B. Tissera, M. S. Alonso, and G. Coldwell, *Mon. Not. Roy. Astron. Soc.*, **346**, 1189, 2003.
4. C. Li, G. Kauffmann, T. M. Heckman et al., *Mon. Not. Roy. Astron. Soc.*, **385**, 1903, 2008.
5. S. L. Ellison, D. R. Patton, L. Simard, and A. W. McConnachie, *Astron. J.*, **135**, 1877, 2008.
6. D. W. Darg, S. Kaviraj, C. J. Lintott et al., *Mon. Not. Roy. Astron. Soc.*, **401**, 1552, 2010.
7. D. R. Patton, S. L. Ellison, L. Simard et al., *Mon. Not. Roy. Astron. Soc.*, **412**, 591, 2011.
8. H. S. Hwang, D. Elbaz, J. C. Lee et al., *Astron. Astrophys.*, **522**, A33, 2010.
9. S. L. Ellison, J. T. Mendel, J. M. Scudder et al., *Mon. Not. Roy. Astron. Soc.*, **430**, 3128, 2013.
10. A. R. Petrosian and M. Turatto, *Astron. Astrophys.*, **297**, 49, 1995.
11. T. A. Nazaryan, A. R. Petrosian, A. A. Hakobyan et al., *Astrophys. Space Sci.*, **347**, 365, 2013.
12. J. C. Mihos and L. Hernquist, *Astrophys. J.*, **464**, 641, 1996.
13. P. F. Hopkins, T. J. Cox, L. Hernquist et al., *Mon. Not. Roy. Astron. Soc.*, **430**, 1901, 2013.
14. D. F. Woods and M. J. Geller, *Astron. J.*, **134**, 527, 2007.
15. V. Wild, T. Heckman, and S. Charlot, *Mon. Not. Roy. Astron. Soc.*, **405**, 933, 2010.
16. S. L. Ellison, D. R. Patton, J. T. Mendel, and J. M. Scudder, *Mon. Not. Roy. Astron. Soc.*, **418**, 2043, 2011.
17. X. Liu, Y. Shen, and M. A. Strauss, *Astrophys. J.*, **745**, 94, 2012.
18. A. Dressler, *Astrophys. J.*, **236**, 351, 1980.
19. M. Sol Alonso, D. G. Lambas, P. Tissera, and G. Coldwell, *Mon. Not. Roy. Astron. Soc.*, **367**, 1029, 2006.
20. S. L. Ellison, D. R. Patton, L. Simard et al., *Mon. Not. Roy. Astron. Soc.*, **407**, 1514, 2010.
21. C. Park and Y.-Y. Choi, *Astrophys. J.*, **691**, 1828, 2009.
22. J. M. Scudder, S. L. Ellison, and J. T. Mendel, *Mon. Not. Roy. Astron. Soc.*, **423**, 2690, 2012.
23. M. Sol Alonso, D. G. Lambas, P. Tissera, and G. Coldwell, *Mon. Not. Roy. Astron. Soc.*, **375**, 1017, 2007.
24. T. J. Cox, P. Jonsson, R. S. Somerville et al., *Mon. Not. Roy. Astron. Soc.*, **384**, 386, 2008.
25. J. M. Scudder, S. L. Ellison, P. Torrey et al., *Mon. Not. Roy. Astron. Soc.*, **426**, 549, 2012.
26. D. G. Lambas, S. Alonso, V. Mesa, and A. L. O’Mill, *Astron. Astrophys.*, **539**, A45, 2012.
27. A. A. Hakobyan, A. R. Petrosian, B. McLean et al., *Astron. Astrophys.*, **488**, 523, 2008.
28. S. Kaviraj, S. Peirani, S. Khochfar et al., *Mon. Not. Roy. Astron. Soc.*, **394**, 1713, 2009.
29. P. Di Matteo, F. Bournaud, M. Martig et al., *Astron. Astrophys.*, **492**, 31, 2008.
30. C. K. Xu, D. L. Shupe, M. Béthermin et al., *Astrophys. J.*, **760**, 72, 2012.
31. S. L. Ellison, P. Nair, D. R. Patton et al., *Mon. Not. Roy. Astron. Soc.*, **416**, 2182, 2011.
32. V. Z. Adibekyan and A. R. Petrosian, *Astrophysics*, **52**, 192, 2009.
33. K. R. V. Casteels, S. P. Bamford, R. A. Skibba et al., *Mon. Not. Roy. Astron. Soc.*, **429**, 1051, 2013.
34. D. R. Patton, R. G. Carlberg, R. O. Marzke et al., *Astrophys. J.*, **536**, 153, 2000.

35. P. F. Hopkins, *Mon. Not. Roy. Astron. Soc.*, **420**, L8, 2012.
36. T. A. Nazaryan, A. R. Petrosian, and B. J. McLean, *Astrophysics*, **55**, 448, 2012.
37. B. E. Markarian, V. A. Lipovetsky, J. A. Stepanian et al., *Soobshch. Spets. Astrofiz. Obs.*, **62**, 5, 1989.
38. A. Petrosian, B. McLean, R. J. Allen, and J. W. MacKenty, *Astrophys. J. Suppl. Ser.*, **170**, 33, 2007.
39. C. P. Ahn, R. Alexandroff, C. Allende Prieto et al., *Astrophys. J. Suppl. Ser.*, **203**, 21, 2012.
40. X. Yang, H. J. Mo, F. C. van den Bosch et al., *Astrophys. J.*, **671**, 153, 2007.
41. M. A. Strauss, D. H. Weinberg, R. H. Lupton et al., *Astron. J.*, **124**, 1810, 2002.
42. G. Kauffmann, T. M. Heckman, S. D. M. White et al., *Mon. Not. Roy. Astron. Soc.*, **341**, 33, 2003.
43. J. Brinchmann, S. Charlot, S. D. M. White et al., *Mon. Not. Roy. Astron. Soc.*, **351**, 1151, 2004.
44. J. A. Baldwin, M. M. Phillips, and R. Terlevich, *Publ. Astron. Soc. Pacif.*, **93**, 5, 1981.
45. W. Kollatschny, A. Reichstein, and M. Zetzl, *Astron. Astrophys.*, **548**, A37, 2012.
46. L. C. Ho, *Annu. Rev. Astron. Astrophys.*, **46**, 475, 2008.